Measurements of Solar Occultation: the Error in a Naive Retrieval if the Constituent's Concentration Changes

H. K. ROSCOE
Department of Atmospheric Physics, Clarendon Laboratory, Parks Road, Oxford OX1 3 PU, England

and

J. A. PYLE
Department of Physical Chemistry, Lensfield Road, Cambridge CB2 1EP, England

Abstract. The stratospheric concentrations of many minor constituents change rapidly at sunrise or sunset. If this happens, there is an inherent error when retrieving the vertical profiles of the constituents from measurements of their absorption of sunlight. For retrievals of NO at sunset the error can be estimated from *in-situ* measurements alone, without appeal to a model of stratospheric photochemistry. Below 20 km this error can approach 100% so that the retrieved NO is zero. But at 40 km, and at 25 km when the absorption is strong and Lorentzian, it can be less than 20%. Precise calculations of the error, even if small, require model calculations of the sunset and sunrise changes. With a model, we have calculated the error for NO, NO_2, OH and ClO.

1. Introduction

A common method of determining the concentration of a minor constituent in the stratosphere is to observe its absorption of sunlight at sunrise or sunset from a satellite or a balloon. Such a measurement of solar occultation has high sensitivity because of the long absorbing paths of the sun's rays through the atmosphere, and its signal-to-noise ratio is large because of the high intensity of the sun.

The curvature of the Earth causes most of the absorption to occur at the lowest point in the path (the tangent height). By measuring the absorption at several tangent heights during an occultation, the vertical profile of the constituent's concentration can be retrieved. This is often done by determining the concentration high in the atmosphere and working downwards, a procedure
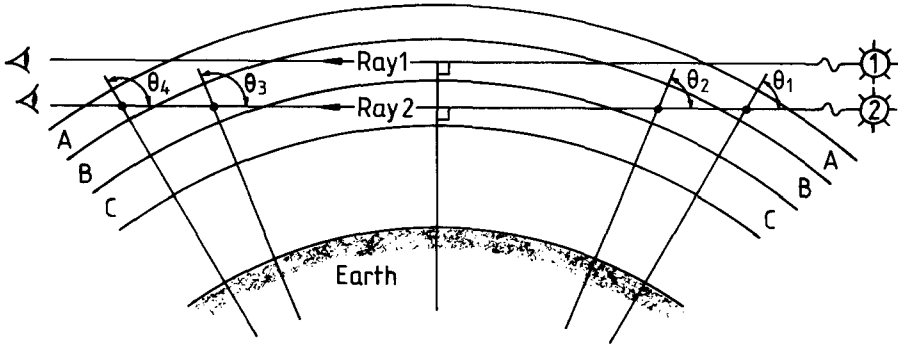
Fig. 1. Geometry of a solar occultation measurement from a satellite. The concentration in layer B is deduced by observing ray 1. To deduce the concentration in layer C from ray 2, the absorption in layer B must be known. But ray 2 is observed at a different time to ray 1, and the concentration in layer B may have changed. Note that θ_2 and θ_3 are equally displaced from 90°.

known as 'onion peeling'. Unfortunately, if the concentration changes rapidly near sunrise or sunset, the retrieval process contains an inherent error: in order to deduce the concentration at the tangent height, the concentration at higher altitudes must be known, but it has changed since it was measured.

Figure 1 illustrates the problem for an instrument on a satellite. When the sun is at position 2, ray 2 traverses layers A, B and C. The absorption in layers A and B must be subtracted from the total absorption to deduce the concentration in layer C. But the concentration in layer B was deduced from ray 1, when the solar zenith angle was 90° in layer B; in ray 2 the angles θ_2 and θ_3 are not 90°, so the solar time in layer B is different – the concentration has changed. A retrieval of the concentration profile which does not take account of this change, one which we choose to call a naive retrieval, is in error.

An alternative retrieval scheme is to find a best fit between calculated and measured absorptions using all the data at once, retrieving the profile at all altitudes simultaneously. Although we have described the nature of the retrieval error in terms of onion-peeling, the error is in fact the same with either scheme.

Previous papers by Boughner et al. (1980), by Kerr et al. (1977), and by Vaughan (1982) have discussed this error for retrievals of NO and ClO, of NO_2, and of mesospheric O_3, respectively. They showed that the error was usually less than 25% at 30 km, and negligible at 40 km. Unfortunately their work appears to have been widely ignored because they did not show the geometry of the rays and the time dependence of the concentrations in a way that could be easily understood by nonspecialists in retrieval theory; and because, by linking their calculations to computer models of stratospheric chemistry, their conclusions seemed to depend on their chosen model. In this paper we show the nature of the error in an occultation retrieval in a way that

we hope is clear even to the nonspecialist, and show the probable size of this error for NO without appeal to a model. We also show how to take account of the pressure and temperature dependences of the absorption when calculating the error. In Section 3, by using a model which is refined to fit measurements of the change in NO at sunset, we calculate detailed errors in retrievals of NO, NO_2, OH, and ClO – constituents which cover a range of diurnal variations.

Solar occultation retrievals refer to a solar zenith angle of 90°. The change in concentration between noon and 90° is quite a different issue to the retrieval error we discuss here.

2. Errors in Retrievals from Measurements of Solar Occultation

In Figure 1, simple geometry shows that the sums of $\theta_2 + \theta_3$ and of $\theta_1 + \theta_4$ are 180°. They might, for example, be 88° and 92°, and 87° and 93°. So the average angle of ray 2 in layer B is 90°, the same angle as when the concentration in layer B was measured by ray 1. If the change in concentration in layer B is linear with solar angle, then the average concentration in layer B is the same for ray 2 and ray 1 – there is no retrieval error. So the error depends only on the nonlinearity of the change in the constituent with solar angle.

Note that this conclusion (that the retrieval error is zero if the change is linear with solar angle) is independent of the degree of non-linearity of the absorption as a function of the number of absorbing molecules along the path – the conclusion is still valid if the centres of the lines are opaque (saturated) unless the absorption is measured by a monochromatic (e.g., heterodyne) spectrometer. Such saturation may reduce the sensitivity of the measurement, but a specific equivalent width relates to a specific number of molecules – the line grows wider when there are more molecules in the path. Also the conclusion is independent of the pressure and temperature dependence of the absorption if the pressure and temperature of layer A is assumed to be the same all along the layer (the usual assumption). Although the temperature at a fixed height does vary around the day due to solar heating propagated by gravity waves, even if this were 15 K peak-to-peak the maximum change during the hour of sunset would be 2 K. This is a negligible change for instruments which do not sense atmospheric emission and so are independent of Planck function, and in any case such changes would induce no error if they were linear with solar angle and the absorption was a linear function of temperature.

To take the specific example of NO at sunset, its decay has been measured by Ridley *et al.* (1976) and by Kondo *et al.* (1980). Figure 2 shows their results, and it is clear that the change is not linear. An extreme nonlinearity might be an abrupt fall to zero NO just after a solar angle of, say, 92°, as in Figure 3(a). A worse case for inducing a retrieval error would be if the daytime
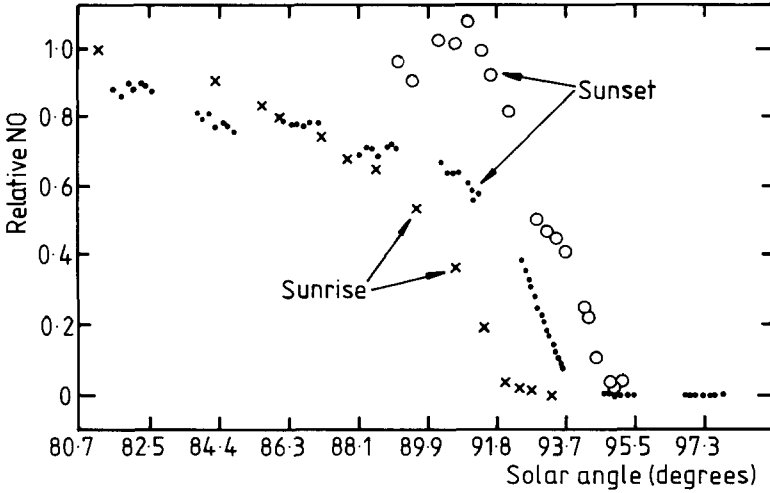
Fig. 2. Measurements of the decay of NO at sunset by Ridley *et al.* (1976) at 34.5 km ($\bigcirc$), and by Kondo *et al.* (1985) near 32 km (.); and of the rise of NO àt sunrise by Ridley *et al.* (1977) at 26.4 km ($\times$). Balloon-borne chemiluminescent samplers measured the NO concentrations. The data of Ridley *et al.* is the ratio of the measured NO to that at a solar angle of 90° (sunset) or 81° (sunrise). The data of Kondo *et al.* is the ratio of the measured NO to that measured at the same altitude during ascent earlier in the day, to take account of a small change in balloon height during the sunset period.
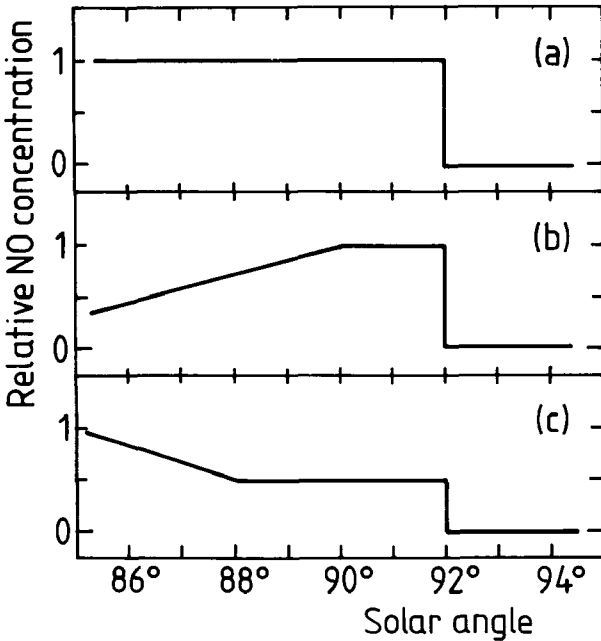

Fig. 3. Changes in NO across sunset which might give greatest errors in a naive retrieval from an occultation measurement. From the text, (b) is the worst case for a satellite measurement; (c) is worse for changes above the balloon in a measurement from a balloon.
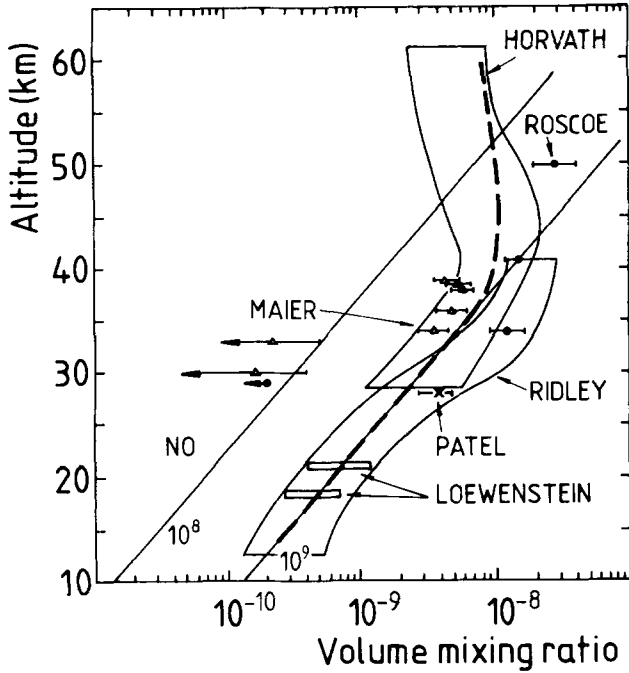
Fig. 4. Measurements of the vertical profile of NO, from WMO (1982). The dashed line shows the profile assumed for calculations discussed in the text.

concentration increased to a maximum at 92° before falling abruptly to zero, similar to Figure 3(b), since the average of concentrations at, say, 93° and 87° would be even less than half that at 90°. However, Figure 2 shows the opposite trend before 90°. So let us assume the change shown in Figure 3(a) as a worst case. Figure 4 shows the daytime profiles of NO measured by several workers. Let us assume the compromise profile of the dashed line in the figure.

Next let us construct a scheme of layer thicknesses which allows easy manipulation of different possible changes of NO with solar angle. If we choose layers whose tops are 1, 4, 9, 16 and 25 km above the tangent point, the solar zenith angles at the layer boundaries are 91, 92, 93, 94 and 95° respectively (the radius of the earth in kilometres and the number of degrees in a radian allow this useful approximation). Despite the inconvenience of different layers for each ray, such a scheme has the further advantage that the path length of the ray through each layer is the same, about 115 km. Figure 5 illustrates the scheme, and the heights of each layer are given in Table I for four rays.

In the table, the concentrations from the dashed profile in Figure 4 are listed for each layer. Figure 7 plots these concentrations along the ray assuming no diurnal variations. If we now assume the diurnal variation shown in

Table I. Heights, concentrations, and errors for NO retrievals. The layer scheme is that of Figure 5, and the concentration profile is the dashed line of Figure 4

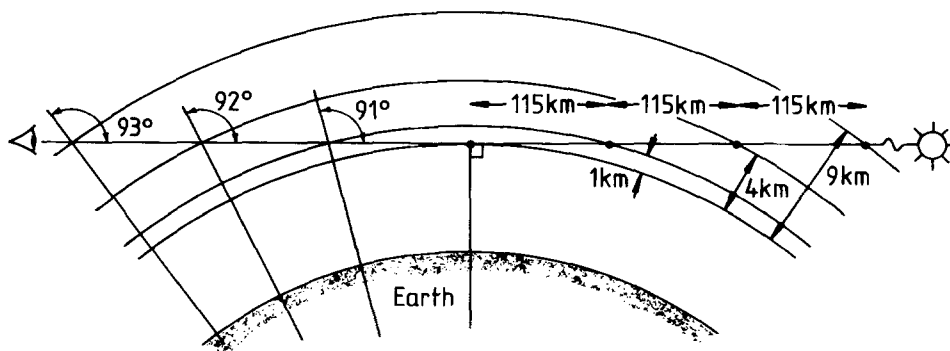| Solar angle at top of layer (deg)	Height of top above tangent (km)	Height of centre above tangent (km)	Tangent height									
			18 km		32 km		40 km		25 km			
			Height (km)	Conc. (10^9)	Height (km)	Conc. (10^9)	Height (km)	Conc. (10^9)	Height (km)	Conc. (10^9)	p (mb)	-0.5 $T^{-1/2}$
91	1	0.5	18.5	1.0	32.5	1.0	40.5	0.7	25.5	1.0	20	0.067
92	4	2.5	20.5	1.0	34.5	1.0	42.5	0.65	27.5	1.0	14	0.066
93	9	6.5	24.5	1.0	38.5	0.9	46.5	0.4	31.5	1.0	8.7	0.065
94	16	12.5	30.5	1.0	44.5	0.55	52.5	0.1	37.5	0.95	3.5	0.064
95	25	20.5	38.5	0.9	52.5	0.1	60.5	–	45.5	0.45	–	0.062
96	36	30.5	48.5	0.2	62.5	–	70.5	–	55.5	0.05	–	0.062
Apparent errors with abrupt falls at												
92° (Fig. 3a)			78%		39%		19%		61%		(20% with p & T weight)	
93°			53%		16%		4%		36%		(7% with p & T weight)	
True errors with abrupt falls at												
92° (Fig. 3a)			36%		30%		19%		36%			
93°			30%		14%		4%		27%			

Fig. 5. The scheme of layers for the calculation in the text of possible errors in the retrieval of NO. This scheme allows the reader to calculate new errors with new assumptions very easily because, along a ray, the segments of path in each layer are equal. Note that the model calculations in Section 3 use a different scheme (layers of thickness 0.5 scale-heights, about 3 km) since those layers are a fundamental property of the model.
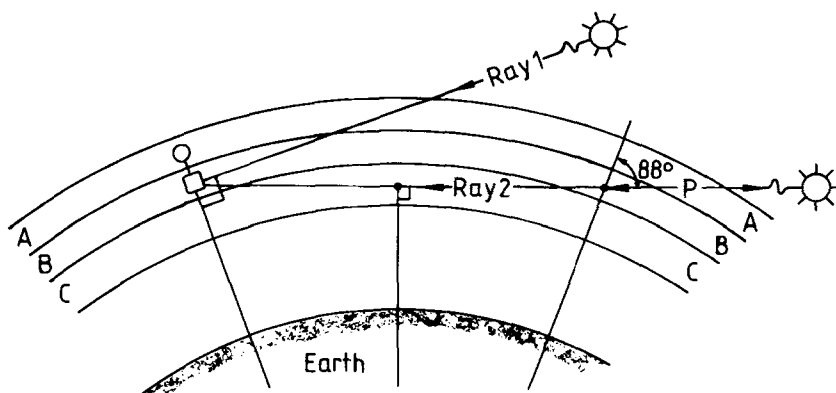

Fig. 6. Geometry of a solar occultation measurement from a balloon. The concentration in layer B is deduced by measuring ray 1. To deduce the concentration in layer C from ray 2, the absorption in layer B must be known, but the solar angle has changed from 90° to 88° in layer B at the time of ray 2.

Figure 3(a), the error can be clearly seen from the hatched area in the figure, due to the spurious absorption assumed in the retrieval for zenith angles greater than 92°. The proportional error is given by the hatched area divided by the amount in the tangent layer (the shaded area). Table I lists these apparent errors both for an abrupt fall in NO to zero at 92°, and for an abrupt fall at 93°.

These are the errors when the equivalent width of the absorption is only dependent on the number of molecules in the path, and is independent of pressure and temperature. This is close to the case for the NO_2 band near 440 nm, and for a weak line near the peak of a P or R branch of a vibration-rotation band in the infrared. In the case of a strong Lorentzian line, the
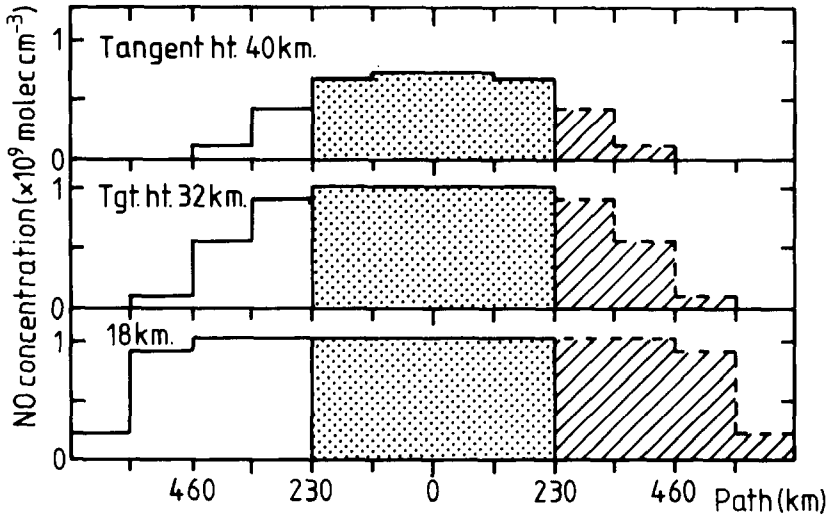
Fig. 7. NO concentrations at the altitudes of Table I, for rays at 3 tangent heights observed from a satellite. The NO profile is the dashed line of Figure 4. The horizontal scale shows the path length of the ray in each layer, so that the area under each line is the amount of NO in each layer that would be seen by an instrument observing that ray. The solid line shows the NO assuming the decay of Figure 3(a). The dashed line shows the NO at solar angle 90° (i.e., no decay). The difference between the two is the hatched area. The apparent proportional error at the tangent height due to a naive retrieval is this difference divided by the amount in the tangent layer (the shaded area), provided the absorption is weak and independent of temperature.

equivalent width depends on $u\,p$ (amount $\times$ pressure). For paths in series, the equivalent width of a line is proportional to:

$$\sqrt{\sum_{\text{all paths}} u\,p}$$

so that each shaded area in Figure 7 must be weighted by pressure. Since the tangent height is at higher pressure than other levels, the error is less than in the case of weak absorption. Similarly, if the Lorentz width is also proportional to $T^{-1/2}$, this weight will increase the shaded areas most at lowest altitudes within the stratosphere, since the temperature is lowest there, and again the error is less. Figure 8 shows the amounts of NO at one tangent height in Figure 5, redrawn with these simple weights. The error reduces from 61 to 20% when the NO falls abruptly at 92°. Although strong Lorentzian absorption is unlikely for NO in the infrared, for NO_2 below 25 km it is very probable. For NO_2 lines near the centre of its band at 1600 cm^{-1}, the temperature dependences of line strengths and widths combine to $T^{-5/2}$, further reducing the error.

The balloon case differs from the satellite case in that there is no compensation for levels above the balloon since these layers are sampled only once: in Figure 1, instead of the mean solar angle in layer B being the average of θ_2 and θ_3 in ray 2, if the balloon is at the base of layer B this mean is just θ_2.

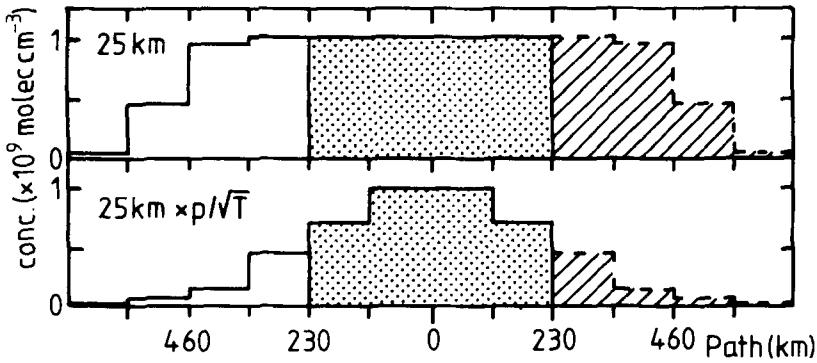Fig. 8. NO concentrations along a ray with tangent height 21 km, as in Figure 7, and the same concentrations weighted by pressure × (temperature)$^{-1/2}$ below 5 mb. These weights are the ones to be expected from strong Lorentzian lines, and significantly reduce the apparent error from the weak absorption case.

In Figure 6, which shows some representative angles for a typical balloon measurement, layer B is, as always, observed at solar angle 90°; but in ray 2 the solar angle in layer B is 88° – always on the daytime side of the terminator. Paradoxically, although at sunset ray 2 occurs later than ray 1, the solar time for ray 2 in layer B is earlier. This means that if the concentration does not change until the sun goes below the horizontal there is no retrieval error due to changes above the balloon. But even a slow linear change which starts when the sun is above the horizontal, as in Figures 3(b) and (c), will introduce an error.

Note that, as at all altitudes in the satellite case, a linear change below the balloon induces no error. But the change above the balloon (path p in Figure 6) induces an error in the concentration retrieved below the balloon, the error being greatest at lowest altitudes. Furthermore, this error due to the change above the balloon is opposite in sign to the error due to the change below the balloon when the change has the form of Figure 3(c). Figure 9 shows the NO concentrations with such a change. The error at 25 km due to the change
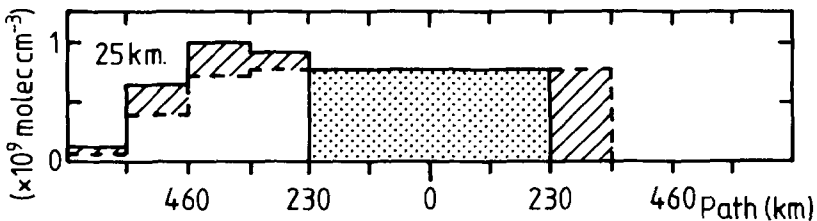

Fig. 9. NO concentrations along a ray at tangent height 25 km for a solar occultation measurement from a balloon at 34 km. The assumed change of NO is that of Figure 3(c). The apparent error is now the difference between the left-hand and right-hand hatched areas divided by the shaded area. Note it is smaller than in the satellite case in the upper part of figure 8.
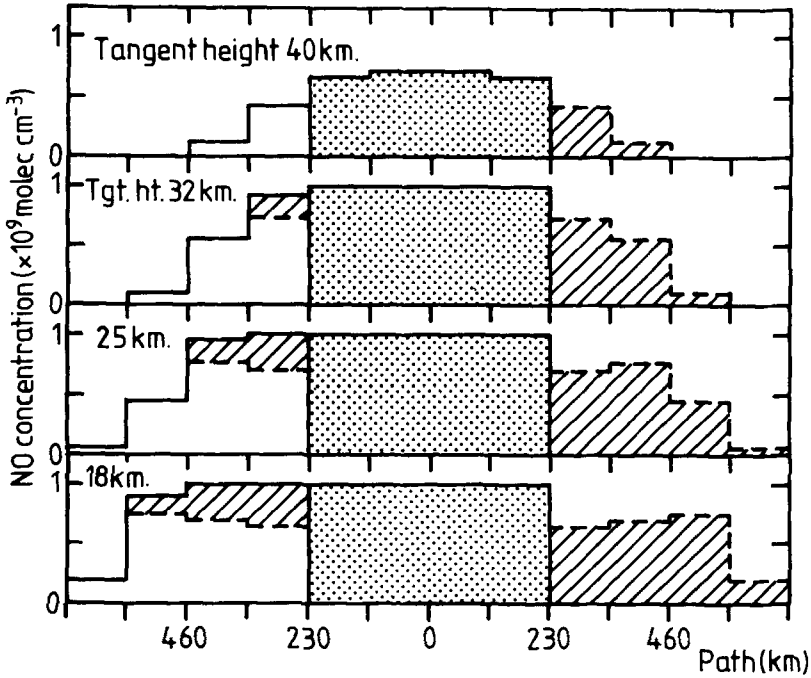
Fig. 10. As in Figure 7, except that the dashed line shows the concentration which has been naively retrieved at layers above the tangent layer. The true error is the difference between the left-hand and right-hand hatched areas, divided by the shaded area. Note that at lower tangent heights the true error is substantially less than the apparent error in Figures 7 and 8.

above the balloon is +12% compensated by an error of −25% due to the change below the balloon, so that the total error is −13%.

Figures 7, 8 and 9 show the error assuming that all concentrations above the tangent layer have been correctly retrieved. Unfortunately this is not usually the case – the retrieved concentrations at these upper levels are also in error. The more realistic (and more complicated) calculation must use the amounts depicted in Figure 10. Here, the error above 40 km was assumed negligible; but along the ray of tangent height 32 km, the amount at 40 km is reduced because the 40 km retrieval was in error. The true error is then less than the apparent error depicted in Figure 7. Along the ray of tangent height 25 km, the amounts at both 32 and 40 km must be reduced, so that the true error at 25 km is proportionately even lower than at 32 km.

Table I lists these true errors at each altitude. In the table, the true error becomes constant below 25 km, whereas the apparent error mushrooms rapidly to over 50%. The stability of the true error as one goes down in altitude is clearly an artefact of the constant concentration assumed in Figure 4 – if the concentration of NO were much lower at 20 km than at 30 km, the true error would still be very large below 20 km. For example, if the concen-

tration between 30 and 37 km were 2×10^9 and that below 23 km were 0.5×10^9, instead of 1×10^9 everywhere (entirely possible from Figure 4) the errors below 20 km would be increased to 100% for an abrupt fall in NO at 92°. In this case the sign of the error is such that a naive retrieval would deduce zero NO. Again, Figure 2 shows that at sunrise the NO does not reach half its high-sun value until 90.5°. If this were approximated to an abrupt change at 91°, it is clear from Figure 11 that the error would be much larger and could easily reach 100% even with concentrations close to the uniform 1×10^9. Note that the nonlinear shape of the change in NO at sunrise is similar to that at sunset in Figure 2, but it has a greater effect at sunrise because it occurs closer to 90°. So the sign of the error is the same despite time moving in opposite directions at sunrise to sunset in Figure 2 – it is the change with solar angle, not with time, that defines the error.

Note that the tangent amount when calculating this error (the shaded areas in the figures) is not just the amount in the first layer (of thickness 1 km) but is more nearly the amount in the lower two layers (of combined thickness 4 km). This is because the vertical resolution of a realistic satellite sensor of modest signal-to-noise ratio is the half-width of the natural weighting function (about 3 km) convolved with the vertical field of view. If the sensor had very high signal-to-noise ratio so that differences could be taken between adjacent fields, a vertical resolution of 2 km might be achieved. In this case the path in the appropriate tangent layer would be reduced by a factor 1.4, and the percentage errors would be greater by a factor 1.4. Interestingly, the error due to sunrise and sunset changes seems to depend on the vertical resolution of the retrieved profile.

3. Model Predictions

The discussions of Section 2 show that model calculations of the errors in a retrieval must be treated with caution – the error depends on the profile, the vertical resolution of the measurement, the pressure and temperature dependence of the absorption, and on how faithfully the model calculates the nonlinearity of the sunrise or sunset changes. Present instruments which measure the constituents we discuss here would not claim an absolute accuracy of better than 30%, but exact retrievals for future, more accurate instruments must incorporate the change of concentration as a function of solar angle into the retrieval scheme, as pioneered by Boughner *et al.* (1980). Nevertheless, calculations with theoretical profiles, resolutions, and pressure dependences give useful insight.

In this study, we have calculated concentrations with the photochemical model of Fabian *et al.* (1981). This diurnal model was recently updated by Roscoe *et al.* (1986). A preliminary calculation failed to produce the measured behaviour of NO at sunset – the predicted decrease occured at the terminator,

later than the measured decrease. In the model, scattered light is parameterised in a way based on the detailed work of Lacis and Hansen (1974). For solar angles below the horizontal, there was no scattering, just absorption. The scheme was modified to include Rayleigh scattering using coefficients tabulated by Nicolet (1984). Figure 11 shows the much improved agreement between prediction and measurement when this modified scattering scheme was included. Unfortunately NO is the only photochemically active gas for which we have measurements at high time resolution, but the good agreement in Figure 11 gives faith in the accuracy of model predictions of the changes in other constituents.

We have predicted the concentrations of four constituents across sunrise and sunset. Figures 12 to 17 show their changes, and Table II lists the errors for each constituent. The skewness of some of the figures shows the effect of the nonlinear changes in a very dramatic way, and allows the reader to see at a glance which altitudes are responsible for the greater part of the errors and what effects different profiles to those predicted by the model would have on the errors. Note that although the error for NO depends, as described in Figure 12, on the difference between left- and right-hand hatched areas, if the concentration were to change as in Figure 3(b), the error would depend on the sum of the left- and right-hand hatched areas.

The table reproduces for all molecules the features deduced for NO in Section 2 from measurements and simple geometry: the error is greatest at lowest altitudes, and it is greater at sunrise than at sunset. Again, as in Section 2, a naive retrieval underestimates NO and overestimates NO_2, and it can
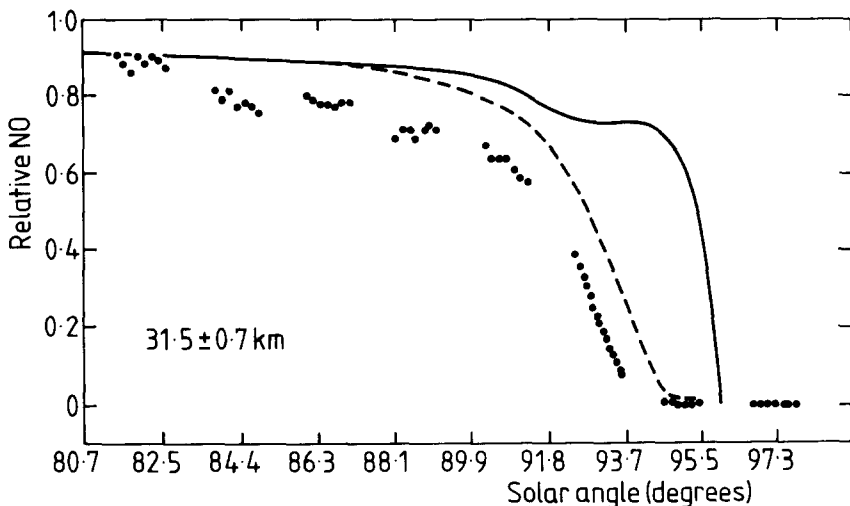

Fig. 11. Measurements of NO by Kondo *et al.* (1985) with a chemiluminescent sonde (points), compared to predictions by the model of Fabian *et al.* (1981) (solid line), and by the model with improved Rayleigh scattering (dashed line).

Table II.   Model calculations of the percentage error in the concentration of constituents measured by solar occultation from a satellite, when the retrieval of the profile ignores rapid changes in the concentration during the period of sunrise or sunset. The calculation assumes the absorption to be weak. OH is unsuitable for measurement at the lower altitudes because of its low concentration there

Tangent height (km)	Sunset or sunrise	NO	NO_2	ClO	OH
18.6	SS	−61	+8	−12	−
24.9	SS	−15	+7	−14	−
24.9	SR	−55	+12	+58	−
31.5	SS	−5	+2	0	−6
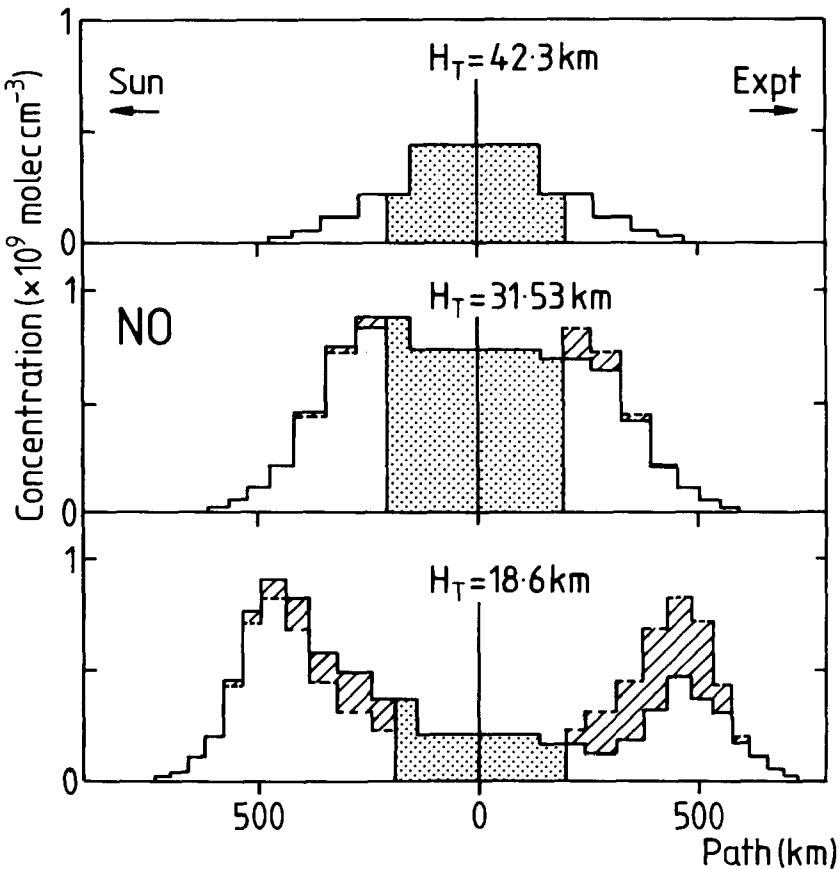
Fig. 12.   Model predictions of the NO concentrations at sunset at altitude intervals of 0.5 scale-heights (approx. 3 km), for rays at 4 tangent heights. The horizontal scale shows the path length of the ray in each layer, so that the area under each line is the amount of NO in each layer that would be seen by an instrument observing that ray. The solid line shows the predicted NO at the solar angle of the ray in each layer. The dashed line shows the predicted NO at solar angle 90°. For weak absorption, the error at the tangent height due to a naive retrieval is the hatched area on the left of the tangent point, minus the hatched area on the right, divided by the amount in the tangent layer (shaded).
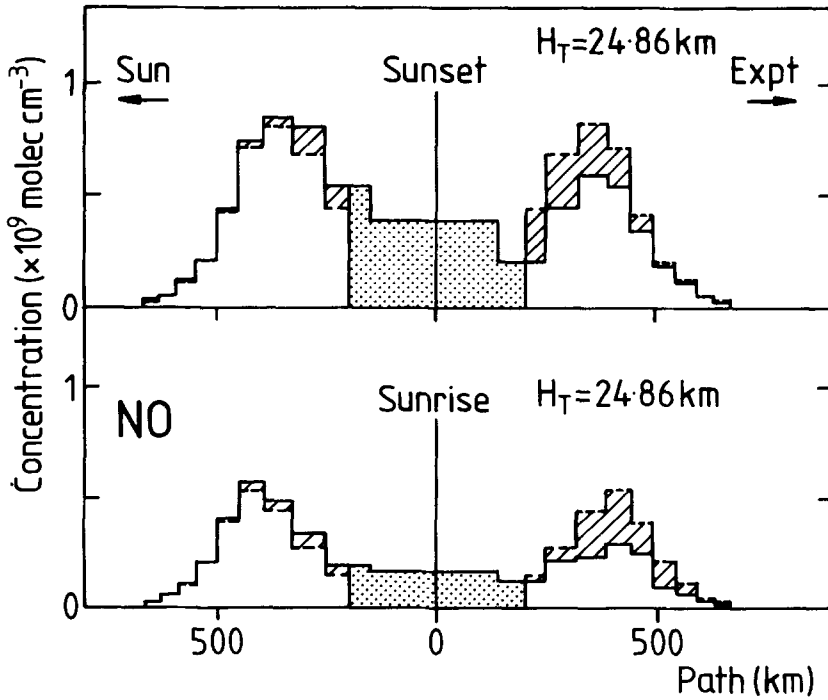
Fig. 13.   As Figure 12 but for NO at sunrise and at sunset, at one tangent height.

deduce zero or negative NO below 25 km at sunrise. ClO is an interesting case because it does not have a very rapid change just at sunrise or sunset, but at 25 km the error can still be large because of the modest concentration there compared to higher altitudes, and because the change is significantly nonlinear with solar angle. Although at 31 km OH is also dwarfed by the

Table III.   Calculated equivalent widths of groups of NO_2 lines for a limb ray at sunset with tangent height of 24.9 km. The NO_2 profile was calculated by the model, but in some cases extra NO_2 was added to the tangent layers. Units are cm^{-1}. The apparent error in a naive retrieval of NO_2 is deduced by linear interpolation of the calculated equivalent widths.

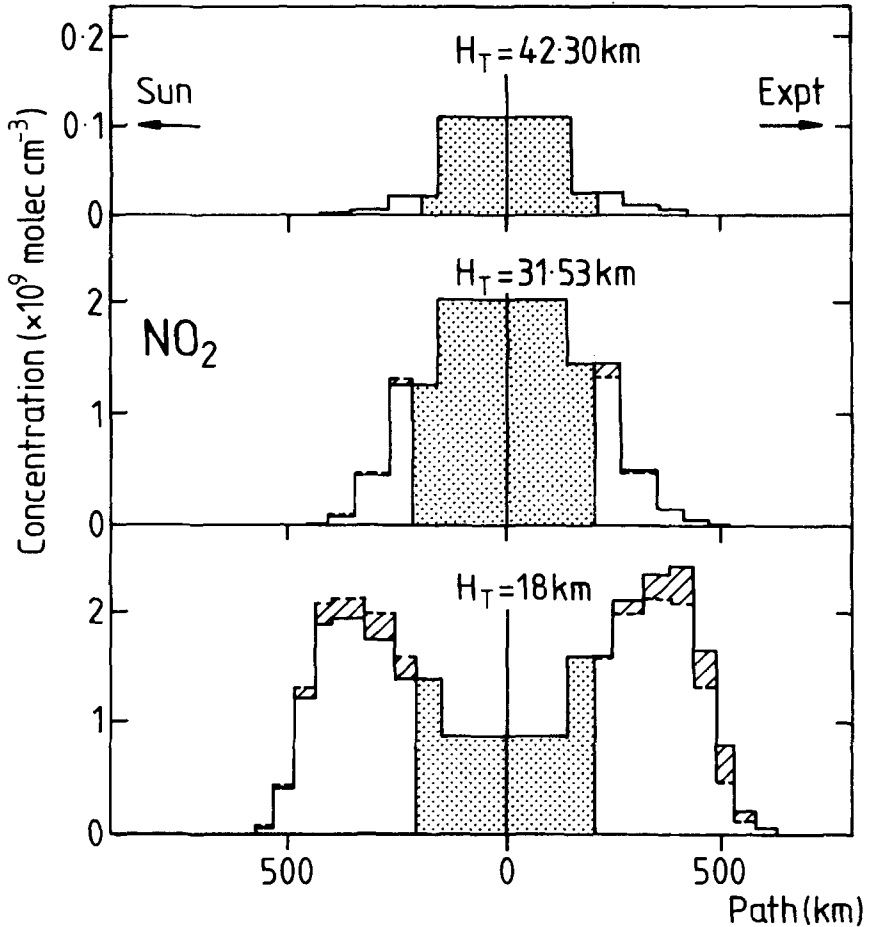| Solar angles	Amount added to tgt. layer	1604.1 to 1604.7 cm^{-1}	1605.1 to 1605.5 cm^{-1}	1605.9 to 1606.4 cm^{-1}
true	0	0.07821	0.06362	0.08120
90°	0	0.07709	0.06261	0.07993
90°	+5%	0.07830	0.06365	0.08116
90°	+10%	0.07952	0.06466	0.08235
apparent error in retrieved NO_2		4.63%	4.86%	5.17%

Fig. 14.   As Figure 12 but for NO_2.

column above, the calculated changes are extremely linear with solar angle, so the error is quite small.

Of these molecules, only NO_2 is likely to have absorption lines which are strong and Lorentzian. With a line-by-line program, we have calculated the equivalent widths of groups of NO_2 lines in the infrared band near 1600 cm^{-1}. The occultation error for NO_2 is of special interest to the 1983 Balloon Inter-comparison Campaign (Roscoe et al. 1984), and we chose the groups of lines used by the Grille spectrometer in that campaign (Louisnard et al. 1983). Table III lists these equivalent widths at one tangent height. From the table, the change in equivalent width is nearly linear in concentration for changes in concentration of up to 10%, and the error is similar but not identical for each group of lines, as predicted above. Note that the apparent error is only about 5%, instead of about 10% when the absorption is weak.
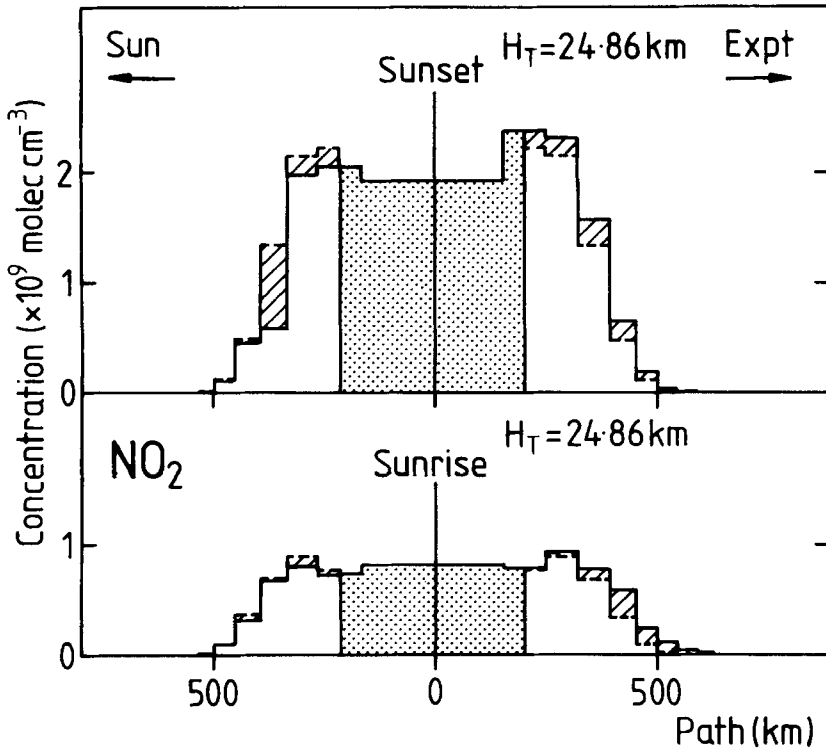
Fig. 15.   As Figure 12 but for NO_2 at sunrise and at sunset, at one tangent height.

We emphasise that the errors listed in Table II depend on the predicted profile – these errors cannot be added uniformly to a naively retrieved profile to determine the true profile.

Finally, we stress again that the error introduced in solar occultation retrievals of satellite data, due to changes in concentration near sunrise or sunset, is caused by the nonlinearity of these changes with solar zenith angle. The retrieval can be improved by including a model of these changes, but this is only appropriate if the model can be shown to be accurate during this difficult period. Only for NO are the detailed observations available; for other constituents we cannot yet reliably assess the models for this purpose.

Acknowledgements
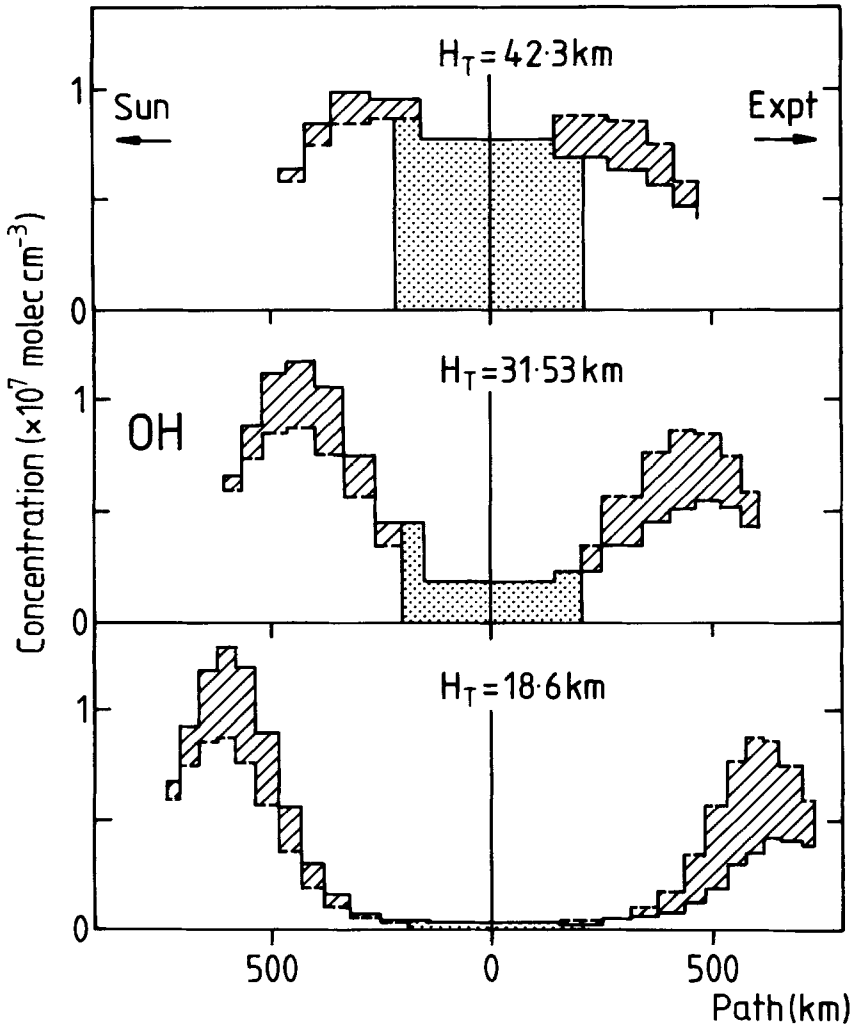
Fig. 16.   As Figure 12 but for OH.

References

Boughner, R., Larsen, J. C., and Natarajan, M., 1980, The influence of NO and ClO variations at twilight on the interpretation of solar occultation measurements, *Geophys. Res. Lett.* 7, 231.

Fabian, P., Pyle, J. A., and Wells, R. J., 1982, Diurnal variation of minor constituents in the stratosphere modelled as a function of latitude and season, *J. Geophys. Res.* 87, 4981–5000.
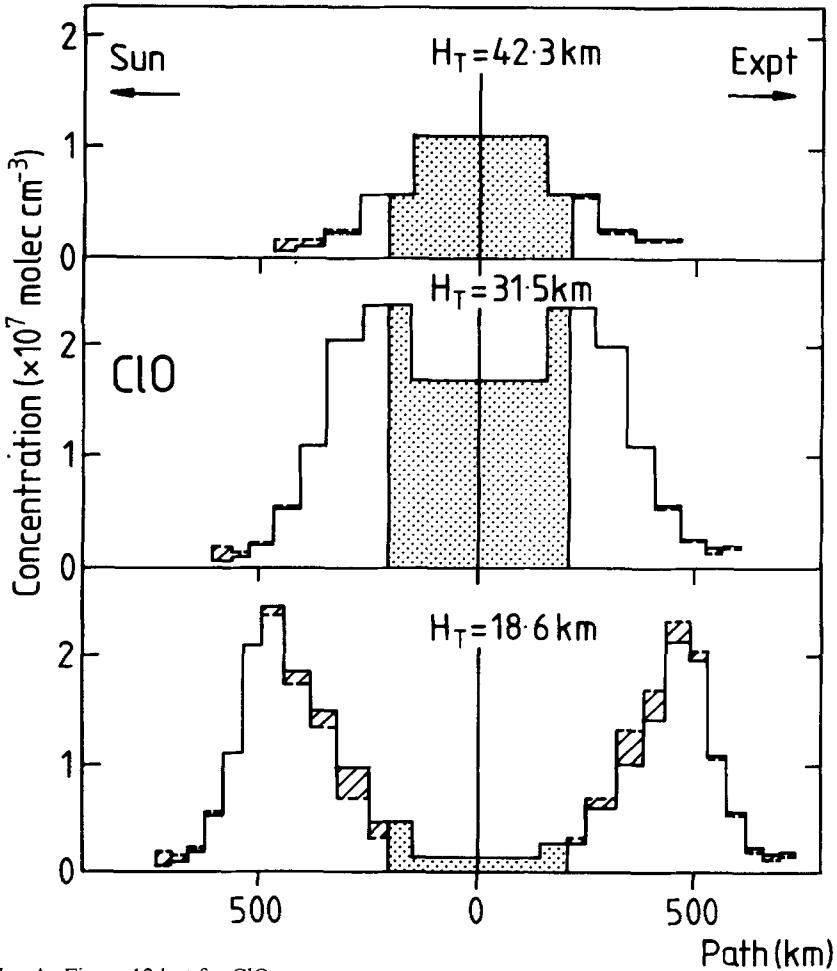
Fig. 17.   As Figure 12 but for ClO.

Kondo, Y., Matthews, W. A., Iwata, A., and Takagi, M., 1984, Measurement of nitric oxide from 7 to 32 km and its diurnal variation in the stratosphere, *J. Geophys. Res.* **90**, 3813.

Kerr, J. B., Evans W. F. J., and McConnell, J. C., 1977, The effects of NO_2 changes at twilight on tangent ray NO_2 measurements. *Geophys. Res. Lett.* **4**, 577.

Lacis, A. A. and Hansen, J. E., 1974, A parameterisation for the absorption of solar radiation in the earth's atmosphere, *J. Atmos. Sci.* **31**, 118–133.

Louisnard, N., Fergant, G., Girard, A., Gramont, L., Lado-Bordowsky, O., Laurent, J., Le Boiteux, S., and Lemaitre, M. P., 1983, Infrared absorption spectroscopy applied to stratospheric profiles of minor constituents, *J. Geophys. Res.* **88**, 5365–5376.

Nicolet, M., 1984, On the molecular scattering in the terrestral atmosphere: an empirical formula for its calculation in the homosphere, *Aeron. Act.* No. 284.

Ridley, B. A., Bruin, J. T., Schiff, H. I., and McConnell, J. C., 1976, Altitude profile and sunset decay measurements of stratospheric nitric oxide, *Atmosphere* **14**, 180.

Ridley, B. A., McFarland, M., Bruin, J. T., Schiff, H. I., and McConnell, J. C., 1977, Sunrise measurements of stratospheric nitric oxide, *Can. J. Phys.* **55**, 212.

Roscoe, H. K., Kerridge, B. J., Pollitt, S., Bangham, M., Louisnard, N., Alamichel, C., Pommereau, J.-P., Ogawa, T., Iwagami, N., Coffey, M. T., Mankin, W., Flaud, J.-M., Camy-Peyret, C., Murcray, F. J., Goldman, A., Evans, W. F. J., and McElroy, T., 1984, Intercomparison of stratospheric measurements of NO and NO_2, *Proc. Ozone Symposium, Greece*, pp. 149–150.

Roscoe, H. K., Kerridge, B. J., Gray, L. J., Wells, R. J., and Pyle, J. A., 1986, Simultaneous measurements of stratospheric NO and NO_2 and their comparison with model predictions, *J. Geophys. Res.* **91**, 5405–5420.

Vaughan, G., 1982, Mesospheric ozone, Oxford University DPhil Thesis.

WMO, 1982, The stratosphere 1981, theory and measurements, WMO global ozone research and monitoring project, Report No. 11.